

Dynamic corrosion of copper-nickel sulfide by *Acidithiobacillus ferrooxidans*

TONG Lin-lin(佟琳琳), JIANG Mao-fa(姜茂发), YANG Hong-ying(杨洪英),
YU Juan(俞娟), FAN You-jing(范有静), ZHANG Yao(张耀)

School of Materials and Metallurgy, Northeastern University, Shenyang 110004, China

Received 3 April 2008; accepted 16 October 2008

Abstract: The dynamic corrosion process of bio-oxidation of copper-nickel sulfide from Karatungk in northern Xinjiang Province of China was studied. The polished wafer of the copper-nickel sulphide was used to carry on a series of oxidation corrosion experiment by *Acidithiobacillus ferrooxidans*. The changes of superficial corrosion appearance and the mineral dynamic corrosion process were discovered by microscope observation. Then, the galvanic cell model was established, and the bio-oxidation activation order of typical copper-nickel sulphide minerals was ascertained as pyrrhotite > pentlandite > chalcocopyrite.

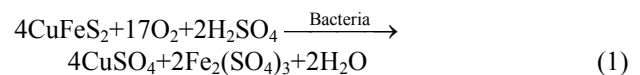
Key words: copper-nickel sulphide; bio-oxidation; dynamic corrosion; galvanic effect

1 Introduction

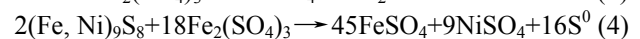
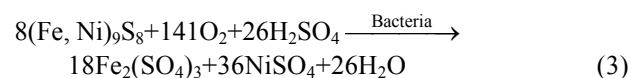
Bio-oxidation is an advanced technique of mineral processing. This method has become the research interest of hydrometallurgy in recent years[1–5]. Previous researches of bio-oxidation were mainly focused on breeding of dominant bacteria[6–8], influence of bio-oxidation, optimization and control of leaching process[9–10] and bio-metallurgical processes of different mineral by bacteria. In fact, the bio-oxidation system involves interface problems such as bacterial/mineral and mineral/mineral[11], so researching the surface morphology changes can help us to reveal oxidation mechanism of bio-oxidation. Chalcocopyrite is the most common copper sulfide in the copper-nickel ores. The oxidation of the secondary copper sulfide was easy but that of the primary copper sulfide was difficult, so secondary copper sulfide (chalcocite, covellite, etc.) was applied in bio-oxidation at present, while the primary copper sulfide (chalcocopyrite) was still treated with pyrometallurgical method[12]. Resource of chalcocopyrite is widely distributed in nature, but it is difficult to treat with bio-oxidation. The purpose of this work is to show the characteristics of dynamic corrosion of the typical copper-nickel sulfide mineral pairs from the microscopic point of view.

The mechanisms in bio-oxidation of chalcocopyrite and the main associated minerals, pentlandite and pyrrhotite, were obtained. Direct and indirect bio-oxidation reactions in bacterial oxidation process of chalcocopyrite, pentlandite and pyrrhotite take place as follows[13–14]:

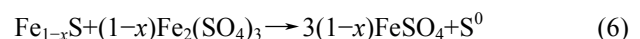
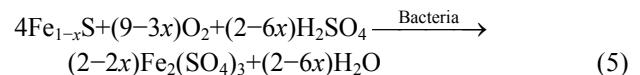
Chalcocopyrite:



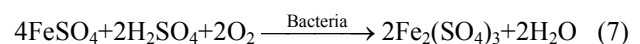
Pentlandite:



Pyrrhotite:



Oxidation of Fe^{2+} :



Oxidation of S^0 :



Foundation item: Project(2006AA06Z127) supported by the National Hi-tech Research and Development Program of China; Projects(50674029, 50274024) supported by the National Natural Science Foundation of China; Project(20060145015) supported by Doctoral Program Foundation of Ministry of Education of China; Project(20052030) supported by the Natural Science Foundation of Liaoning Province, China

Corresponding author: JIANG Mao-fa; Tel: +86-24-83680373; E-mail: jiangmf@smm.neu.edu.cn

DOI: 10.1016/S1003-6326(08)60292-7

2 Experimental

2.1 Mineral samples

The mineral samples for this research were collected from Karatungk copper-nickel sulfide mineral belt in northern Xinjiang of China. Chalcopyrite (molecular formula CuFeS_2) and pentlandite (molecular formula $(\text{Fe}, \text{Ni})_9\text{S}_8$) were the most important minerals in the copper-nickel sulfide. At the same time, they often co-exist with pyrrhotite (molecular formula Fe_{1-x}S , generally $x=0\pm 0.223$, range of corresponding composition $\text{FeS}-\text{Fe}_{11}\text{S}_{12}$)[15].

2.1.1 Mineral testing methods

The mineral species was identified using Leica DMRXP polarized optical microscope by process mineralogy method. EPMA-1600 electron probe micro-analysis (EPMA, SHIMADZU, Institute of Metal Research, Chinese Academy of Sciences) was applied to studying the mineral compositions. The conditions of full spectrum scanning qualitative analysis were as follows: accelerating voltage 15 kV, beam current 10 nA, count time 10 s, beam diameter 20 μm , and analyzer crystals RAP, PBST, PET and LiF. The conditions of spectrum quantitative analysis were as follows: accelerating voltage 15 kV, beam current 10 nA, count time 10 s and beam diameter 20 μm , analyzer crystal of PET for S with FeS_2 as the standard sample, and analyzer crystal of LiF for Co, Fe, Ni with pure Cu as the standard sample, respectively.

2.1.2 Mineral species and compositions

Identification with process mineralogy method shows that the mineral mainly contains metal sulfides of pentlandite (Pe), pyrrhotite (Pyr), chalcopyrite (Cp) and gangue minerals of chrysolite, pyroxene, biotite and plagioclase.

Regions of chalcopyrite, pentlandite and pyrrhotite identified by process mineralogy method were analyzed by electron probe micro-analysis. Fig.1 shows the result of qualitative analysis. There were elements Fe, S, Ni and Co in the region of pentlandite, elements Fe, S, and Cu in the region of chalcopyrite and elements Fe, S, and Ni in the region of pyrrhotite. Table 1 lists the result of quantitative analysis.

2.2 Bacterial sample

Acidithiobacillus ferrooxidans (A.f) were used in experiment. Culture medium was 9K liquid medium ($(\text{NH}_4)_2\text{SO}_4$ 3 g/L, KCl 0.1 g/L, K_2HPO_4 0.5 g/L, $\text{MgSO}_4 \cdot 7\text{H}_2\text{O}$ 0.5 g/L, $\text{Ca}(\text{NO}_3)_2$ 0.01 g/L, $\text{FeSO}_4 \cdot 7\text{H}_2\text{O}$ 44.2 g/L), adjusted to pH 1.80 with 2 mol/L sulfuric acid. Before experiment, activated culture was conducted to bacteria for three times, and the concentration was above 10^8 cell/mL.

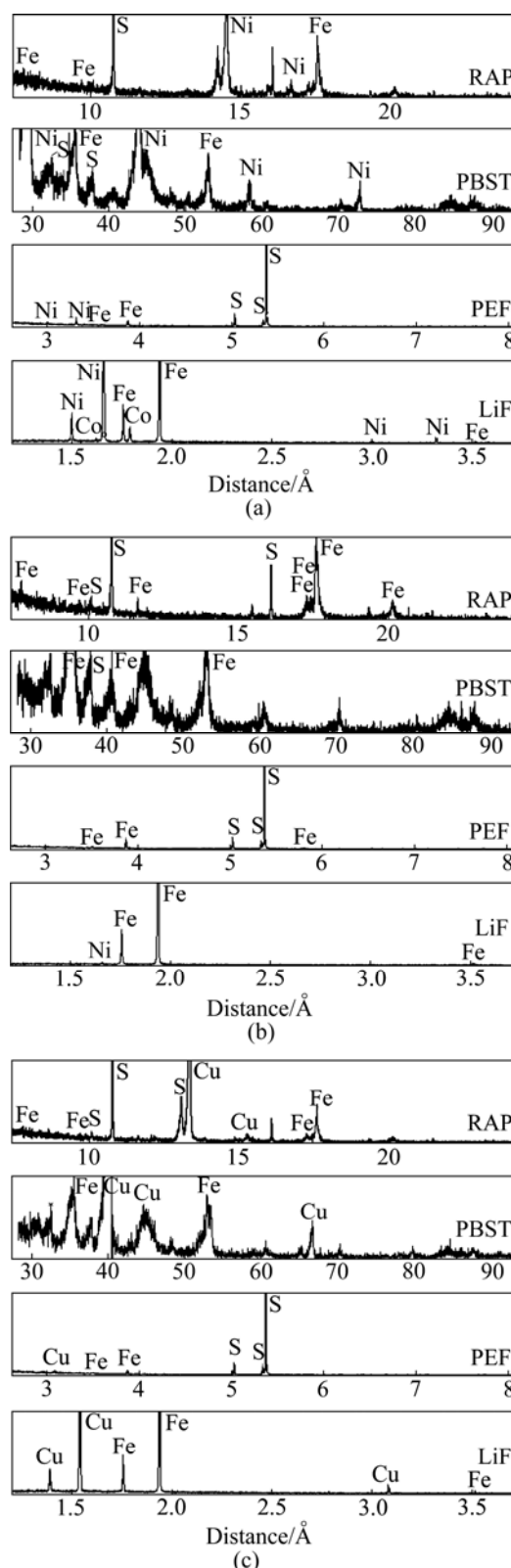


Fig.1 Results of qualitative analysis by EPMA: (a) Pentlandite; (b) Pyrrhotite; (c) Chalcopyrite

This experiment was carried out in a 3 L tank with a mechanic agitator at 950 r/min. When bacteria grow into stationary phase, minerals were added into tank with

initial potential of 590 mV and initial pH of 1.8. The certain field of minerals was observed by Germany Leica DMRX microscope at a certain time interval.

3 Results

3.1 Dynamic corrosion process of bio-oxidation of pyrrhotite/chalcopyrite mineral pair

In the bio-oxidation corrosion experiment, pyrrhotite and chalcopyrite showed a sharp contrast. Before bio-oxidation, pyrrhotite crystal surface was smooth in pinkish brown and strong metallic luster. Chalcopyrite crystal surface was smooth in brass yellow and strong metallic luster. After the bio-oxidation, their microscopic characteristics were changed obviously, as shown in Fig.2.

Pyrrhotite and chalcopyrite showed different oxidation behaviors in the process of bio-oxidation, as listed in Table 2.

3.2 Dynamic corrosion process of bio-oxidation of pyrrhotite/chalcopyrite/pentlandite mineral pairs

Before bio-oxidation, pyrrhotite crystal surface was smooth in pinkish brown and strong metallic luster; pentlandite crystal surface was smooth in light milk

yellow and strong metallic luster; and chalcopyrite crystal surface was smooth in brass yellow and strong metallic luster. After the bio-oxidation, their microscopic characteristics were changed obviously, as shown in Fig.3.

Pyrrhotite, chalcopyrite and pentlandite showed different oxidation behaviors in the process of bio-oxidation, as listed in Table 3.

4 Discussion

4.1 Analysis of bio-oxidation pyrrhotite/chalcopyrite mineral pair

The experiment showed that oxidation rate of pyrrhotite was much faster than chalcopyrite. This was consistent with the view of GOTTSCHALK et al[16] that one sulfide will be significantly oxidated because of different static potentials, while the other will be protected for galvanic effect. In acidic solution, when two sulfides of different static potentials contacted, mineral of high static potential as the cathode will be protected[17–22]. Static potentials obtained by Tafel polarization curves of chalcopyrite, pentlandite and pyrrhotite in bacterial system of three kinds of minerals were 0.318, 0.326 and 0.352 mV, respectively, that is

Table 1 Results of quantitative analysis by EPMA

Mineral	Point number	w(Fe)/%	w(S)/%	w(Ni)/%	w(Cu)/%	w(Co)/%	w(Total)/%	Crystal system
Pentlandite	5	30.736 0	31.978 4	34.594 2	–	2.215	99.422 6	Isometric system[13]
Pyrrhotite	5	60.884 8	37.350 2	0.440 4	–	–	98.674 6	Hexagonal system[13]
Chalcopyrite	5	30.686 2	32.079 6	–	34.904 4	–	97.670 4	Tetragonal system[13]

Table 2 Dynamic corrosion process of bio-oxidation of pyrrhotite/chalcopyrite mineral pair

Oxidation time/h	Change of mineral morphology	
	Pyrrhotite	Chalcopyrite
0	Pyrrhotite crystal surface was clean and smooth with strong metallic luster and pinkish brown color	Chalcopyrite crystal surface was clean and smooth with strong metallic luster, brass yellow of reflected color and weak heterogeneity
24	Metallic luster almost disappeared, reflected color from pinkish-brown to rust, crack significantly deepened with rough surface	Small corrosive pits appeared on surface of chalcopyrite crystal and it was covered in oxidated color
48	Oxidation was very severe, reflected dark color in black and surface cracks became not obvious	Oxidated color was thin, small corrosive pits increased, and crystal periphery oxidation was obvious
72–168	Mineral surface had no change and deep oxidation continued	Reflected color became dark, crack further deepened, and crystal periphery oxidation further strengthened
244	Mineral surface had no change and deep oxidation continued	Oxidation was very severe, reflected color was darker, and surface had red-brown oxidation spots
288	Mineral surface had no change and deep oxidation continued	Oxidation was more severe, reflected color continued to become dark, and red-brown spots of surface became more obvious

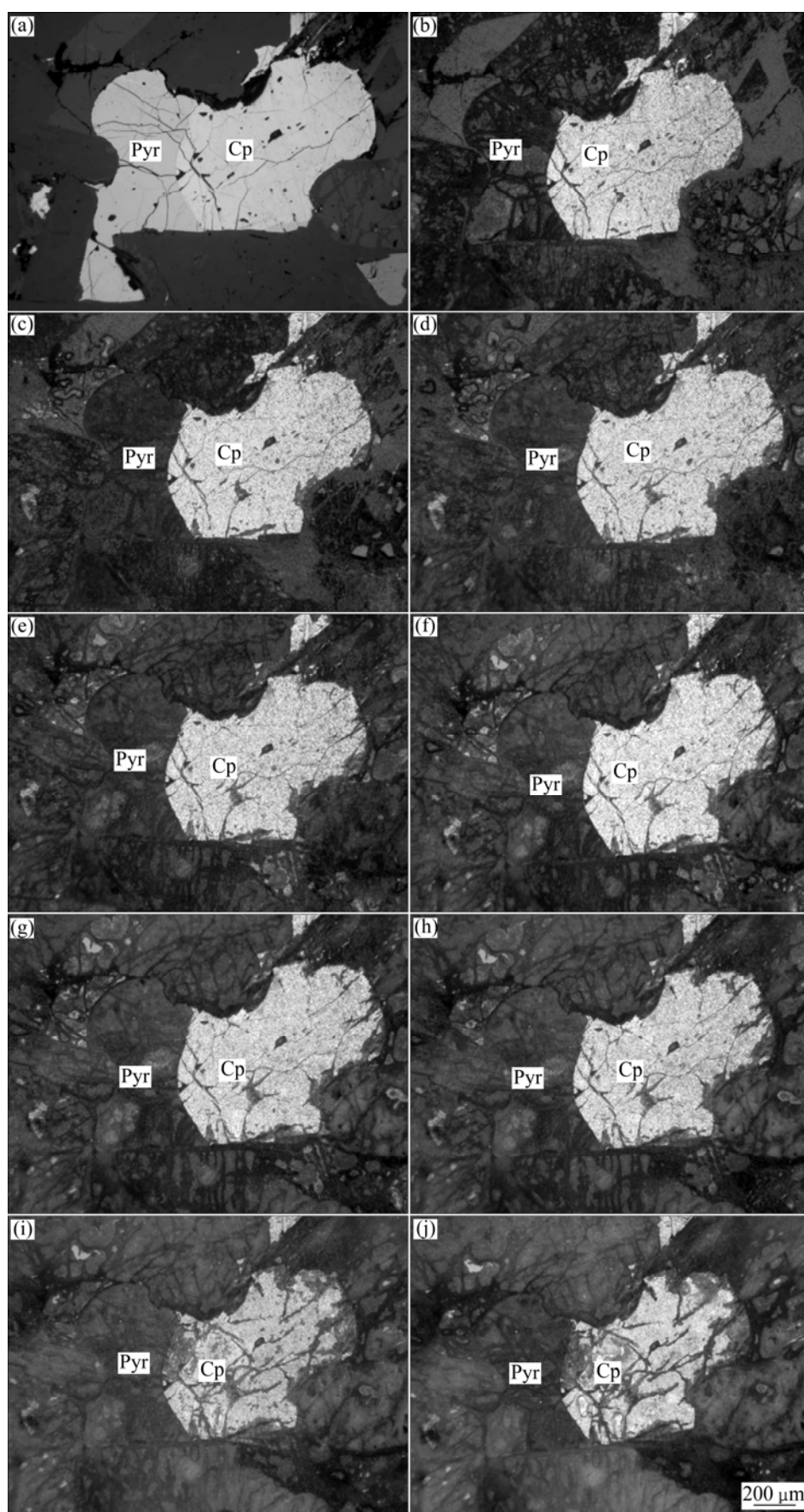


Fig.2 Microscopic characteristics of Pyr/Cp mineral pair after bio-oxidation: (a) 0 h; (b) 24 h; (c) 48 h; (d) 72 h; (e) 96 h; (f) 120 h; (g) 144 h; (h) 168 h; (i) 244 h; (j) 288 h

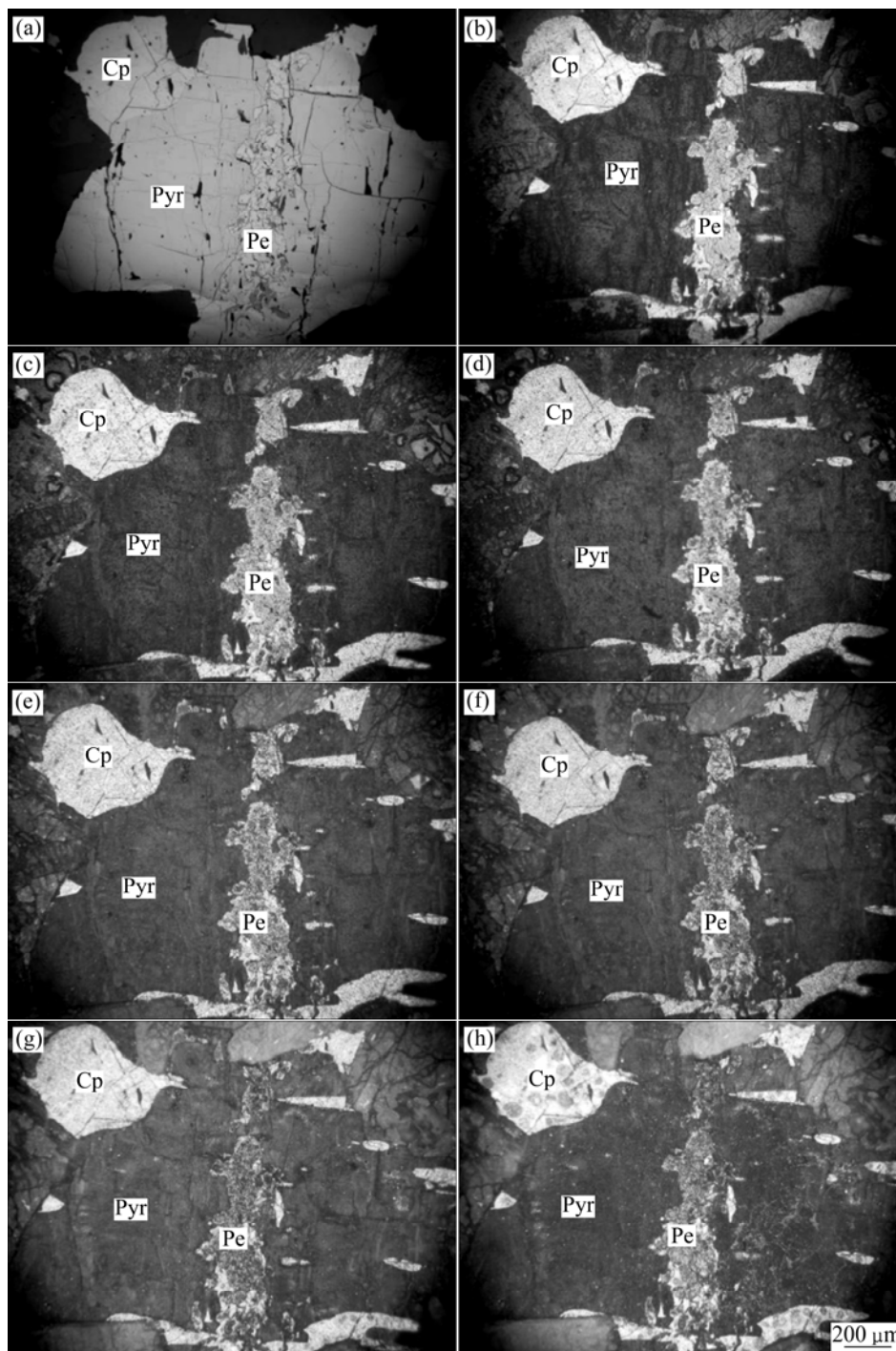


Fig.3 Microscopic characteristics of Pyr/Cp/Pe mineral pairs after bio-oxidation: (a) 0 h; (b) 24 h; (c) 48 h; (d) 72 h; (e) 96 h; (f) 120 h; (g) 192 h; (h) 288h

$\varphi_{Cp} > \varphi_{Pe} > \varphi_{Pyr}$ (Equipment: Shanghai Chenhua Equipment Company: CHI660C Electrochemical workstation). According to the operating principle of galvanic cell, redox reaction occurred on the two poles of cell, and some cations in electrode and the electrolyte solution carried through chemical reaction. Galvanic cell model of pyrrhotite/chalcopyrite mineral pair in bio-oxidation is drawn in Fig.4.

In the bio-oxidation system, pyrrhotite and chalcopyrite formed an galvanic cell. Pyrrhotite had

strong electrochemical activity as anode on which oxidative and corrosiveness occurred. Comparatively, chalcopyrite had strong electrochemical inertia as cathode which was protected. The reaction equations are as follows:

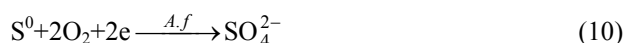
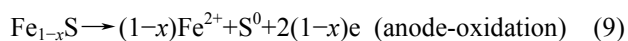
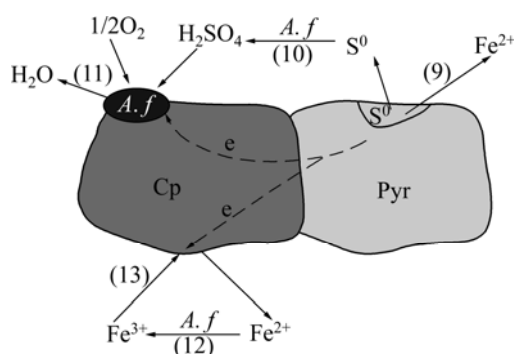


Table 3 Dynamic corrosion process of bio-oxidation of pyrrhotite/chalcopyrite/pentlandite mineral pairs

Oxidation time/h	Mineral morphology change		
	Pyrrhotite	Pentlandite	Chalcopyrite
0	Pyrrhotite crystal surface was clean and smooth in pinkish brown and strong metallic luster	Pentlandite crystal surface was clean and smooth in light milk yellow and strong metallic luster	Chalcopyrite crystal surface was clean and smooth, with strong metallic luster, brass yellow of reflected color, and weak heterogeneity
24	Metallic luster almost disappeared, reflected color turned from pinkish brown to color of rust, crack significantly deepened with rough surface	Small corrosive pits appeared on surface of pentlandite crystal and it was covered in oxidated color	Small corrosive pits appeared on surface of chalcopyrite crystal and it was covered in oxidated color
48	Oxidation was very severe, reflected color was dark in black and surface cracks became not obvious	Oxidation color was thin, and small corrosive pits increased	Oxidation color was thin, and small corrosive pits increased
72–96	Mineral surface had no change and deep oxidation continued	Oxidation color was thin, and small corrosive pits increased	Reflected color turned to darken, and oxidation was further strengthened
120	Mineral surface had no change and deep oxidation continued	Oxidation was very severe, reflected color was dark in black and deep oxidation continued	Reflected color turned to darken, and oxidation was further strengthened
192	Mineral surface had no change and deep oxidation continued	Oxidation was very severe, reflected color was dark in black and deep oxidation continued	Reflected color turned to darken, and oxidation was further strengthened
288	Mineral surface had no change and deep oxidation continued	Oxidation was very severe, reflected color was dark in black and deep oxidation continued	Oxidation was more severe, reflected color continued to turn to dark, and red-brown spots of surface became more obvious

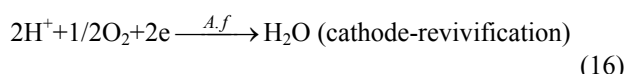
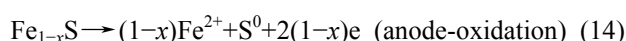
**Fig.4** Galvanic cell model of pyrrhotite/chalcopyrite mineral pairs in bio-oxidation

A. f were absorbed to the surface of chalcopyrite, strengthened electron behavior of O_2 , and Fe^{2+} produced from pyrrhotite was oxidated to Fe^{3+} by bacteria. Fe^{3+} got electron on the surface of chalcopyrite. Fe^{3+} , as oxidant, strengthened the dissolution of pyrrhotite. Furthermore, elemental sulfur produced from pyrrhotite was oxidated to SO_4^{2-} by bacteria, which reduced the clag of the production layer on the surface for the dissolution of pyrrhotite.

4.2 Bio-oxidation pyrrhotite/chalcopyrite/pentlandite mineral pairs analysis

In process of oxidation of pyrrhotite/chalcopyrite/pentlandite mineral pairs, three minerals had different static potentials, and formed galvanic cell. Galvanic cell model of pyrrhotite/chalcopyrite/pentlandite mineral pairs in bio-oxidation is drawn in Fig.5.

In the bio-oxidation system, there were two galvanic cells. Pyrrhotite and chalcopyrite formed an galvanic cell, and pyrrhotite and pentlandite formed the other one. Pyrrhotite worked as anode, and chalcopyrite and pentlandite worked as cathode. Reaction equations were as follows:



A. f were absorbed to the surfaces of chalcopyrite and pentlandite, strengthened electron behavior of O_2 , and Fe^{2+} produced from pyrrhotite was oxidated to Fe^{3+}

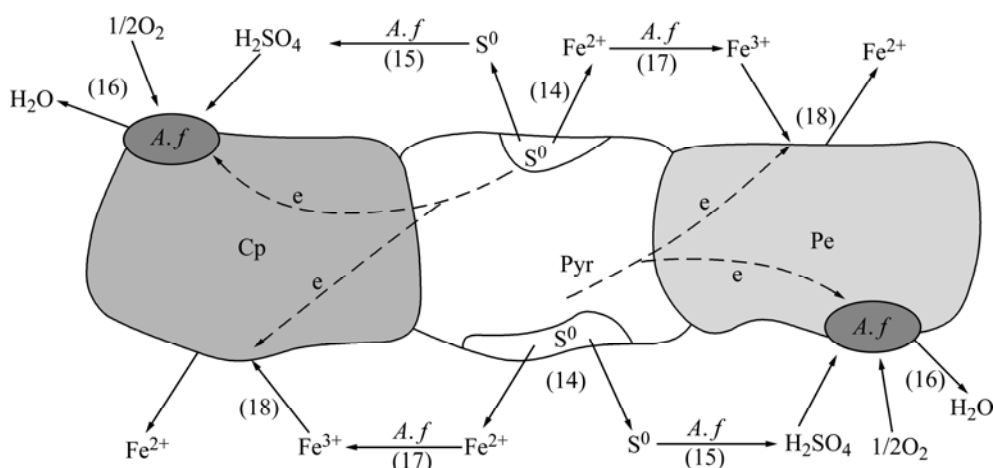


Fig.5 Galvanic cell model of pyrrhotite/chalcopyrite/pentlandite mineral pairs in bio-oxidation

by bacteria. Fe^{3+} got electron on the surfaces of chalcopyrite and pentlandite. Fe^{3+} , as oxidant, strengthened the dissolution of pyrrhotite. Furthermore, elemental sulfur produced from pyrrhotite was oxidated to SO_4^{2-} by bacteria, which reduced the clog of the production layer on the surface for the dissolution of pyrrhotite.

4.3 Comparison of bio-oxidation rate of main sulfides

The bio-oxidation corrosion experiment results showed that pyrrhotite was the most easily oxidized mineral, pentlandite was moderate, and chalcopyrite was the hardest in copper-nickel sulfide from Karatungk. Bio-oxidation rate of main sulfide was in the order of pyrrhotite > pentlandite > chalcopyrite.

5 Conclusions

1) Bio-oxidation rate of pyrrhotite was the fastest among the three minerals, which came after by pentlandite, and the slowest was chalcopyrite. Bio-oxidation rate sequence of main sulfide from Karatungk was pyrrhotite > pentlandite > chalcopyrite.

2) In dynamic corrosion process of bio-oxidation of pyrrhotite/chalcopyrite mineral pair, pyrrhotite and chalcopyrite formed an galvanic cell, with pyrrhotite worked as anode, and chalcopyrite worked as cathode.

3) In dynamic corrosion process of bio-oxidation of pyrrhotite/chalcopyrite/pentlandite mineral pairs, there were two galvanic cells. Pyrrhotite and chalcopyrite formed an galvanic cell, while pyrrhotite and pentlandite formed the other one. Pyrrhotite was anode, chalcopyrite and pentlandite were cathodes.

References

[1] KUMARI A, NATARAJAN K A. Development of a clean

- bioelectrochemical process for leaching of ocean manganese nodules [J]. Minerals Engineering, 2002, 15(1/2): 103–106.
- [2] NESTOR D, VALDIVIA U, CHAVES A P. Mechanisms of bioleaching of a refractory mineral of gold with *Thiobacillus ferrooxidans* [J]. International Journal of Mineral Processing, 2001, 62(1/4): 187–198.
- [3] KUMARI A, NATARAJAN K A. Electrochemical aspects of leaching of ocean nodules in the presence and absence of microorganisms [J]. International Journal of Mineral Processing, 2002, 66(1/4): 29–47.
- [4] MAZUELOS A, PALENCIA I, ROMERO R, RODRÍGUEZ G, CARRANZA F. Ferric iron production in packed bed bioreactors: Influence of pH, temperature, particle size, bacterial support material and type of air distributor [J]. Minerals Engineering, 2001, 14(5): 507–514.
- [5] LIU Z, BORNE F, RATOUCHEK J, BONNEFOY V. Genetic transfer of IncP, IncQ and IncW plasmids to four *Thiobacillus ferrooxidans* strains by conjugation [J]. Hydrometallurgy, 2001, 59(2/3): 339–345.
- [6] LI Hong-xu, DONG Qing-hai, CANG Da-qiang, WANG Dian-zuo. Thermophilic microorganism *Sulfolobus* growth and leaching chalcopyrite properties [J]. Journal of University of Science and Technology Beijing, 2007, 29(1): 20–24. (in Chinese)
- [7] WANG Jian-wei, WANG Mo-hui, YUAN Yuan. The research situation on leaching of ores using mixed bacteria [J]. Multipurpose Utilization of Mineral Resources, 2007(5): 24–27. (in Chinese)
- [8] HALLBERG K B, DOPSON M, LINDSTRÖM E B. Arsenic toxicity is not due to a direct effect on the oxidation of reduced inorganic sulfur compounds by *Thiobacillus caldus* [J]. FEMS Microbiology Letters, 1996, 145(3): 409–414.
- [9] WANG Ying-ru, ZHONG Kang-nian, WEI Yi-he. Optimization of biooxidation pretreatment process of hard-to-leach gold ore [J]. Metal Mine, 2003(10): 40–49. (in Chinese)
- [10] CHEN Shi-guan. Bioleaching and its application in nonferrous metallurgy [J]. Shanghai Nonferrous Metals, 2000, 21(3): 137–146. (in Chinese)
- [11] LIU Jian-she, WANG Zhao-hui, GEN Mei-mei, QIU Guan-zhou. Progress in the study of polyphase interfacial interactions between microorganism and mineral in bio-hydrometallurgy [J]. Mining and Metallurgical Engineering, 2006, 26(1): 40–44. (in Chinese)
- [12] LI Ji-bi. Application status of process for copper hydrometallurgy in domestic and abroad [J]. Hydrometallurgy of China, 2007, 26(1): 13–16. (in Chinese)
- [13] SHU Rong-bo, RUAN Ren-man, WEN Jian-kang. Review on passivation of chalcopyrite during bioleaching process [J]. Chinese

- Journal of Rare Metals, 2006, 30(3): 395–400. (in Chinese)
- [14] DENG Jing-shi. Studies on moderate thermophile intensifying pentlandite leaching [D]. Kunming: Kunming University of Science and Technology, 2002: 11–12. (in Chinese)
- [15] PAN Zhao-lu. Crystallography and mineralogy [M]. Beijing: Geological Press, 1994: 28–34. (in Chinese)
- [16] GOTTSCHALK V, BUEHLER H. Oxidation of sulfides [J]. Econ Geol, 1910, 5: 28–35.
- [17] BERRY V K, MURR L E, HISKEY J B. Galvanic interaction between chalcopyrite and pyrite during bacterial leaching of low-grade waste [J]. Hydrometallurgy, 1978, 3(4): 309–326.
- [18] MEHTA A P, MURR L E. Fundamental studies of the contribution of galvanic interaction to acid-bacterial leaching of mixed metal sulfides [J]. Hydrometallurgy, 1983, 9(3): 235–256.
- [19] WOODS R. Recent advances in electrochemistry of sulfide mineral flotation [J]. Trans Nonferrous Met Soc China, 2000, 10(s1): 26–29.
- [20] MAHMOOD M N, TURNER A K. The selective leaching of zinc from chalcopyrites-phalerite concentrates using slurry electrodes [J]. Hydrometallurgy, 1985, 14(3): 317–329.
- [21] SANTOS L R G, BARBOSA A F, SOUZA A D, LEÃO V A. Bioleaching of a complex nickel-iron concentrate by mesophile bacteria [J]. Minerals Engineering, 2006, 19(12): 1251–1258.
- [22] CRUZ R, LUNA-SÁNCHEZ R M, LAPIDUS G T, GONZÁLEZ I, MONROY M. An experimental strategy to determine galvanic interactions affecting the reactivity of sulfide mineral concentrates [J]. Hydrometallurgy, 2005, 78(3/4): 198–208.

(Edited by YANG Bing)